

The optical and electrical properties exhibited by most of the amorphous semiconductors compared with their single-crystal forms were reviewed by Stuke [11]. In view of these properties the low value of conductivity and the low activation energy of region I, observed for Zn_3P_2 films in our investigation, may be attributed to the disorder in the material due to dangling bonds produced during evaporation. The other possibility of attributing them to the presence of impurities in the material is unlikely in view of the fact that the activation energy in this temperature range, for the impurity-doped samples, is always reported to be higher (0.4 to 0.8 eV) [7]. Thus, the thin films of zinc phosphide studied in this investigation have exhibited all the features that are normally observed in amorphous semiconductors, i.e. a higher value of activation energy in the intrinsic region (greater than the optical band-gap which is about 1.2 eV [5]) and a relatively small influence due to impurity atoms in the extrinsic region.

References

1. R. N. BHARGAVA, *IEEE Trans. Electron Devices* **22** (1975) 691.
2. A. A. BERGH and P. J. DEAN, *Proc. IEEE* **60** (1972) 156.
3. M. G. CRAFT and W. O. GROVES, *ibid.* **61** (1973) 862.
4. W. ZDANOWICZ and L. ZDANOWICZ, *Ann. Rev. Mater. Sci.* **5** (1975) 301.
5. V. V. SOBOLEV and N. N. SYRBU, *Phys. Stat. Sol. (b)* **64** (1974) 423.
6. R. C. SCHOONMAKER, A. R. VENKATARAMAN and P. K. LEE, *J. Phys. Chem.* **11** (1965) 2676.
7. A. MÖLLER, U. ELROD, P. MUNZ, J. HÖNIG-SCHMID, C. CLEMEN and E. BUCHER, 14th International Conference on the Physics of Semiconductors, Edinburgh, 1978, to be published.
8. K. R. MURALI and D. R. RAO, *Sol. Stat. Electron.* **23** (1980) 93.
9. *Idem*, Proceedings of the Nuclear and Solid State Physics Symposium, December, 1978, Publication number 21C (Department of Atomic Energy, Govt of India) p. 217.
10. A. CATALANO, V. DALAL, E. A. FAGEN, R. B. HALL, J. V. MASI, G. WARFIELD and A. M. BARNETT, Proceedings of the International Conference on Photovoltaic Solar Energy, Luxembourg, September, 1977 (D. Reidel Publishing Co., Dordrecht and Boston, 1978) p. 644.
11. J. STUKE, *J. Non. Cryst. Solids* **4** (1970) 1.

Received 22 May

and accepted 13 June 1980

K. R. MURALI
D. R. RAO

Materials Science Centre,
Indian Institute of Technology,
Kharagpur -- 721302,
India

Dependence of defect density and activation energy on deposition rates in copper films

Vacuum evaporated films possess a high value of resistivity compared with that of the bulk because of the incorporation of a large number of defects frozen into the film during atom condensation of the film. The resistivity of the film can be decreased substantially by removing these defects by annealing and ageing. Due to size effects, the resistivity of a very thin annealed film becomes comparable with that of the bulk. Many theories [1–3] have been proposed relating the electrical resistivity with the defects and with the kinetics of their removal during the ageing and annealing processes.

Several investigations [4–10] have been made on different metals and alloys studying the effect

of annealing on the electrical properties of thin films and on the distribution of defect density on various deposition parameters such as residual gas pressure, film thickness, rate of deposition etc. Making use of Vand's theory [1], they studied the lattice vibration energy spectra of the as-grown films. In the present investigation the influence of deposition rate on the defect density $F_0(E)_{\max}$ and activation energy E_{\max} has been studied and discussed on the basis of the sheet resistance of the film before heat treatment.

Copper films of equal thickness (610 Å) were deposited onto well-cleaned glass substrates kept at room temperature. The pressure maintained during the evaporation was $\approx 10^{-5}$ torr. The deposition rate which was changed by altering the heating current through the filament, was estimated making use of a quartz crystal thickness monitor. The film thickness was measured by the

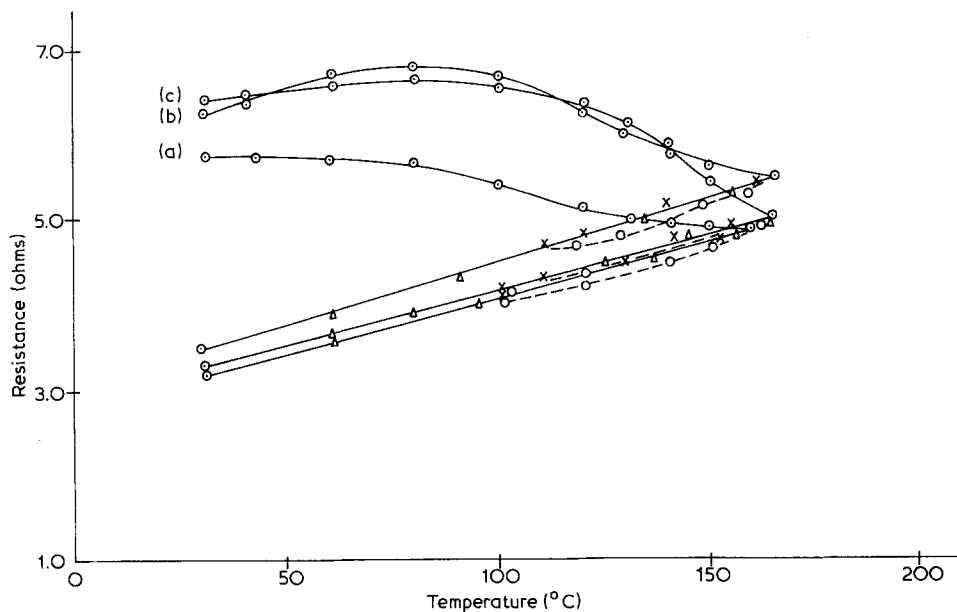


Figure 1 Resistance against temperature plot for copper films (610 Å) formed at different deposition rates during heat treatment: (a) 90 Å min⁻¹; (b) 288 Å min⁻¹; and (c) 630 Å min⁻¹. (○, × heating and cooling for cycle I; △ for cycle II).

Tolansky technique [11]. Without breaking the vacuum, the resistance of the film has been measured with increasing temperature, using a vernier potentiometer having an accuracy of 0.1 μ V. A copper-constantan thermocouple was used for the measurement of temperature during the processes of heating and cooling. The films were subjected to two cycles of heating and cooling and their resistance was continuously measured.

Resistance measurements were carried out at different temperatures, for samples prepared with different deposition rates. The variation of resistance with temperature has been represented in Fig. 1. In the first cycle of annealing the variation of resistance with the increase of temperature at a constant rate (68° Ch⁻¹) follows the general behaviour of most metals. The shape of resistance-temperature curves for the films investigated also indicate the influence of evaporation conditions [12]. The resistance of the films initially either remains constant or increases slightly and then decreases with an increase in temperature. As the increase in resistance due to thermal vibration of the lattice predominates over the decrease in resistance due to the annealing out of defects, which is very small at low temperatures, an increase of resistance with temperature in the

initial stage has been observed as expected. At higher temperatures, the annealing of defects becomes faster and the corresponding decrease in the resistance will be more than the increase of resistance due to the thermal vibration of the lattice, with the result that a net fall in the resistance was noticed. The temperature of the film was increased continuously up to the annealing temperature where the fall of resistance becomes minimum. The film has been cooled from the annealing temperature and during the cooling process the resistance decreases uniformly with temperature as there is only a change in that part of the resistance contributed to by the thermal vibration of the lattice. The defect density remains unaltered below the annealing temperature during the cycling process.

Applying Vand's theory, the lattice distortion energy spectra of copper films for various deposition rates have been calculated and are represented in Fig. 2. Vand suggested that the distortions whose decay is observed during annealing are of the "combined type", i.e. where lattice vacancies and interstitials are in close proximity to one another. The contributions due to the individual lattice vacancies and interstitials in the film are negligible as they can disappear only by long-range

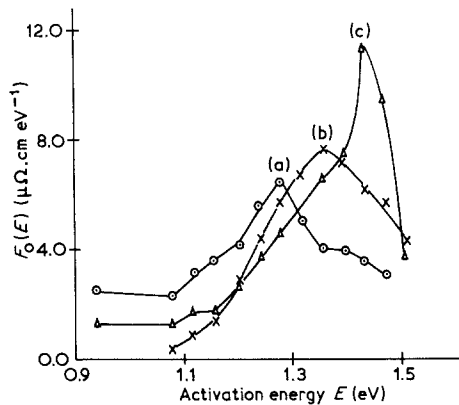


Figure 2 Lattice distortion energy spectra of copper films (610 Å) of different deposition rates: (a) \circ -90 Å min⁻¹; (b) Δ -288 Å min⁻¹ and (c) \times -630 Å min⁻¹.

diffusion to the surface or by chance annihilation upon one type meeting the other [13], whereas the combined type of defect diffuses through short range for their removal which requires only a low activation energy. Hence, the irreversible resistance change observed in the present study is attributed to the distortion of the "combined type". For the elimination of the combined type of defects, the characteristic energy required will be E which can vary from zero all the way to the activation energy for self-diffusion, depending on the structure of the defect [14].

According to Matthiessen's rule, the total resistance of the film $R = R_i + R_T$, where R_i and R_T are the resistances due to impurities and temperatures, respectively. The calculation of the change in the impurity resistivity with the change in temperature (dp_i/dT) during the first cycle of heating has been dealt with in detail elsewhere [9, 10]. For a uniformly rising temperature, for the determination of the distribution function $F_0(E)$ and decay energy E , Vand has shown that $F_0(E) = -1/kU(dp_i/dT)$ and $E = ukT$ where k is a constant and $U = u(u+2)/(u+1)$ [9, 10]. The areas $\int_{E_1}^{E_2} F_0(E) dE$ under the different curves are the contribution to the resistivity by all the defects having decay energies in the specified range. The deposition rate varies from 90 to 690 Å min⁻¹. The $F_0(E)_{\max}$ and E_{\max} values vary from 6.4 to 11.3 $\mu\Omega \text{ cm eV}^{-1}$ and 1.28 to 1.435 eV, respectively. The values of $F_0(E)_{\max}$ and E_{\max} have been found to increase for higher rates of deposition and this is in accordance with the earlier observations [6, 9].

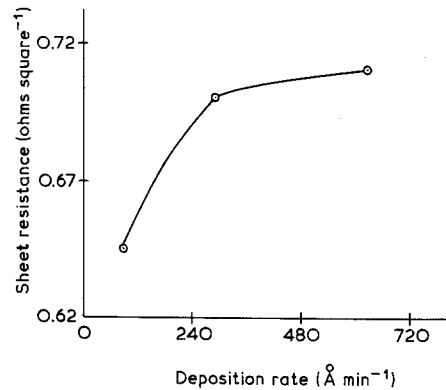


Figure 3 A plot of sheet resistance against deposition rate for copper films (610 Å thickness).

The sheet resistance of the film has been estimated prior to heat treatment in order to provide a satisfactory explanation for the increase of $F_0(E)_{\max}$ and E_{\max} with an increase in deposition rate. A plot of sheet resistance against deposition rate is shown in Fig. 3. It can be clearly seen from the figure that the formation of the defects will increase with the increase of deposition rate and consequently the sheet resistance will also increase. The variation of $F_0(E)_{\max}$ with respect to deposition rate is shown in Fig. 4.

It has been found that the defect density, as well as the activation energy, of copper films increases with an increase in deposition rate and these observations have been explained on the basis of the experimentally obtained sheet resistance data.

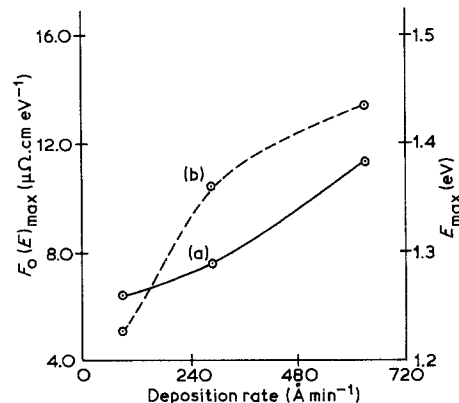


Figure 4 The variation of (a) $F_0(E)_{\max}$ and (b) E_{\max} with deposition rate.

References

1. V. VAND, *Proc. Phys. Soc.* **55** (1943) 222.
2. W. PRIMAK, *Phys. Rev.* **100** (1955) 1677.
3. C. J. MEECHAN and J. A. BRINKMAN, *ibid.* **103** (1956) 1193.
4. J. J. TOYODA and M. NARASHIMA, *J. Phys. Soc. Japan* **14** (1959) 274.
5. P. G. WILKINSON, *J. Appl. Phys.* **22** (1951) 419.
6. V. V. SHAH and Y. G. NAIK, *Indian, J. Pure. Appl. Phys.* **3** (1965) 20.
7. P. G. WILKINSON and L. S. BIRKS, *J. Appl. Phys.* **20** (1949) 1168.
8. M. S. JAGADEESH and V. DAMODARA DAS, *Thin Solid Films* **24** (1974) 203.
9. K. NARAYANDAS, M. RADHAKRISHNAN and C. BALASUBRAMANIAN, *Phys. Stat. Sol. (a)* **56** (1979) 195.
10. *Idem, ibid.* **48** (1978) K71.
11. S. TOLANSKY, "Multiple Beam Interferometry of Surfaces and Films", (Oxford University Press, Oxford, 1948).
12. W. ROMANSKI and D. POTOCZNA PETRU, *Thin Solid Films* **8** (1978) 35.
13. T. J. COUTTS, "Electrical Conduction in Thin Metal Films", (Elsevier Scientific Pub. Co., Amsterdam, Oxford, New York, 1974) p. 184.
14. L. I. MAISSEL and R. GLANC, (Eds) "Handbook of Thin Film Technology" (McGraw-Hill Book Co., New York, 1970) pp. 13–26.

Received 14 May
and accepted 10 June 1980.

K. NARAYANDAS,
M. RADHAKRISHNAN,
C. BALASUBRAMANIAN
*Department of Physics,
Madras University,
Autonomous Post-Graduate Centre,
Coimbatore-641 041,
India*

Electrical conductivity of α-sialon ceramics

A sialon with the α-Si₃N₄ structure, α-sialon, has recently been developed [1–3]. α-sialon ceramics were fabricated by hot pressing or reaction sintering (pressureless sintering). The bending strength and thermal shock resistance were found to be better than those of β-sialons (Si₆₋₂Al₂O₂N₈₋₂) [3].

The general formula for α-sialons may be represented by M_n(Si, Al)₁₂(O, N)₁₆ where M is Li, Mg, Ca, Y or a rare earth metal except La or Ce, and 0 < n ≤ 2. The formula shows that M dissolves in an interstitial site in the α-Si₃N₄ structure [1]. The metal to non-metal ratio in α-sialon, Si + Al/O + N, is always 3/4 as in Si₃N₄ and β-sialon. This means that Al and O atoms dissolve in Si₃N₄ without the formation of vacancies. The maximum number of interstitial sites for metal dissolution in a unit cell of α-sialon is 2. When some of the interstitial sites were occupied, i.e. 0 < n < 2, the rest of the sites could be regarded as vacant sites, through which the diffusion of small ions might be allowed.

The electrical conductivity of β-sialon was very low [4–6]; the application of β-sialons in electric materials was restricted to insulating uses. The structure of α-sialon suggests that sialon ceramics with high electrical conductivity could be prepared.

The present report shows the results of electrical

conductivity measurements of α-sialons and compares them with those obtained for β-sialon.

The sialon ceramics were prepared by hot pressing appropriate powder mixtures [1, 3] to form, (a) Y_{0.41}(Si_{10.2}Al_{1.8})(O_{0.6}N_{15.4}) (α-1), (b) Li₂(Si₉Al₃)(ON₁₅) (α-2), (c) Li_{0.53}Y_{0.20}(Si_{10.3}Al_{1.7})(O_{0.6}N_{15.4}) (α-3), and (d) Si₄Al₂O₂N₆ (β-1). The starting powders were Si₃N₄ (Advanced Material Engineering, England, high purity grade), AlN (Toshiba Ceramics, Japan), Y₂O₃ (Shin-etsu Chemical, Japan, 99.9% pure), Al₂O₃ (Sumitomo Chemical, Japan, AKP-20) and Li₂CO₃ (Junsei Chemical, Japan). The hot pressing was performed at 1700 to 1750°C for 1 h under a pressure of 20 MN m⁻². The porosity of sintered materials was less than 3 per cent. The materials were cut into discs, about 5 mm square and 3 mm thick and then polished. Silver paste electrodes and platinum wires were used as terminals and lead wires, respectively. Platinum paste was also used as the terminal for (α-2) and (α-3) to confirm the agreement in conductivity with that by silver paste at high temperature. The d.c. bridge method was employed in the present work. The measurements were carried out in air in the range room temperature to 980°C.

The electrical conductivities of α- and β-sialons are shown in Fig. 1. The value of (α-1) is about the same as that of (β-1). The values of (α-2) and (α-3), on the other hand, are higher than those of (α-1) and (β-1). The higher conductivities might be